

Small-strain stiffness and deformation behavior of cation crosslinked-xanthan gum treated sand

Dong-Yeup Park^{1a}, Jeong-Uk Bang^{1b}, Minhyeong Lee^{2c}, Ilhan Chang^{3d} and Gye-Chun Cho^{*1},

¹Department of Civil and Environmental Engineering, Korea Advanced Institute of Science and Technology, 291 Daehak-ro, Yuseong-gu, Daejeon 34141, Republic of Korea

²Disposal Safety Evaluation Research Division, Korea Atomic Energy Research Institute, 111 Daedeok-daero 989beon-gil, Yuseong-gu, Daejeon 34057, Republic of Korea

³Department of Civil Systems Engineering, Ajou University, 206 World cup-ro, Yeongtong-gu, Suwon, 16499, Gyeonggi-do, Republic of Korea

(Received February 14, 2025, Revised April 1, 2025, Accepted April 9, 2025)

Abstract. Crosslinked xanthan gum (CrXG) has been introduced to enhance the mechanical stability of biopolymer–soil composites under hydrated conditions. However, its effects on the small-strain stiffness and deformation behavior of granular soils remain underexplored. This study examines the evolution of small-strain shear stiffness, vertical deformation behavior, and shear wave velocity (V_s) in CrXG-treated soils using bender element testing. The results indicate that CrXG treatment improves shear stiffness through a time-dependent gel stiffening mechanism. Higher CrXG concentrations yield greater initial stiffness, with stabilization occurring after approximately 7 days. Additionally, the vertical deformation behavior of CrXG-treated soils is stress-dependent. Increased CrXG concentrations lead to higher V_s values, an elevated α -factor, and a reduced β -exponent, trends that are comparable to those observed in cemented soils. These effects are attributed to the formation of an intergranular hydrogel matrix that enhances particle bonding. These findings provide insights into the mechanical behavior of CrXG-treated soils and their potential applications in geotechnical engineering, particularly for improving soil stiffness and stability.

Keywords: biopolymer; crosslinking; curing time; shear wave; stiffness; vertical stress

1. Introduction

Soil stiffness is a critical parameter in geotechnical engineering, directly affecting the stability and load-bearing capacity of constructions such as tunnels, underground backfills, and levees (Murthy 2002, Park *et al.* 2015, Kim *et al.* 2024). Enhancing stiffness is essential, particularly in soft or loose soils, to support overlying structures and prevent excessive settlement (Budhu 2010). Although cement-based stabilization methods have been widely used to improve ground stability (Liu *et al.* 2022), they pose environmental challenges, including high carbon dioxide emissions and groundwater contamination (Mitchell 2005, Chen *et al.* 2010, Huang *et al.* 2021, Boaventura *et al.* 2023). These concerns necessitate alternative solutions that combine mechanical stability with sustainability (Latifi *et al.* 2017, Bekkouche *et al.* 2022).

Biopolymer-based soil treatment (BPST) has emerged as an eco-friendly and economically viable method for ground reinforcement. Among various biopolymers, xanthan gum (XG) has been extensively studied for its ability to improve compressive strength (Chang *et al.* 2015), shear strength (Lee *et al.* 2017), and permeability control (Bouazza *et al.* 2009, Noh *et al.* 2016, Cabalar *et al.* 2017, Mendonça *et al.* 2020), while also being practically and economically feasible (Chang *et al.* 2020, Seo *et al.* 2021). However, XG develops strength primarily through dehydration, and its performance deteriorates under saturated conditions due to hydrogel swelling and dissolution (Lee *et al.* 2022).

To mitigate these limitations, crosslinked xanthan gum (CrXG) has been developed by incorporating trivalent metal ions to form stable, crosslinked networks. This modification significantly improves the mechanical properties of XG, enabling CrXG to maintain high stiffness and stability even under saturated conditions (Lee *et al.* 2023). Unlike XG, which relies on dehydration (Chang *et al.* 2015, Soldo *et al.* 2020), CrXG gradually increases in stiffness over time via continuous crosslinking, thereby preserving the sustainability of the original biopolymer while enhancing geotechnical engineering properties.

The small-strain shear modulus (G_{max}) is a fundamental parameter that reflects soil stiffness under both dynamic and static loading conditions. It is commonly used to assess the performance and stability of soil structures in applications such as underground constructions (Pitilakis and Tsinidis

*Corresponding author, Assistant Professor

E-mail: gychun@kaist.edu

^aGraduate student

E-mail: dypark2160@kaist.ac.kr

^bGraduate student

E-mail: jeonguk.bang@kaist.ac.kr

^cSenior researcher

E-mail: leemh@kaeri.re.kr

^dAssociate Professor

E-mail: ilhanchang@ajou.ac.kr

2013), road pavements (Anochie-Boateng and Tutumluer 2014), backfills (Bezuijen *et al.* 2005), and reinforced levees (Chakraborty *et al.* 2018). G_{\max} is particularly crucial for predicting ground deformation under dynamic loading scenarios, including seismic events and repetitive fatigue (Atkinson 2000).

G_{\max} is typically determined using soil density (ρ) and shear wave velocity (V_s), which is often measured via laboratory bender element (BE) tests. BE tests are valued for their simplicity and reliability, as shear waves propagate through soil specimens and V_s is computed from wave travel time using the relationship in Eq. (1)

$$G_{\max} = \rho \cdot (V_s)^2 \quad (1)$$

These tests are frequently conducted in K_0 -constrained oedometer cells (where K_0 refers to the coefficient of earth pressure at rest, i.e., the ratio of horizontal to vertical effective stress under no lateral strain conditions) to evaluate the influence of vertical effective stress (Hoyos *et al.* 2015, Oh *et al.* 2017), degree of saturation (Gu *et al.* 2015), and relative density (Salva Ramirez *et al.* 2023, Kim *et al.* 2024) on soil stiffness and deformation behavior. The small-strain deformation behavior of granular soils is significantly influenced by interparticle contact, which can be enhanced by cementation effects. Consequently, BE tests have been extensively applied to assess the effects of cementation on the strength and stiffness of artificially stabilized soils, such as cemented sands, during curing processes and load-induced collapse (Consoli *et al.* 2009, Amaral *et al.* 2011, Ghorbani and Salimzadehshooili 2019).

CrXG hydrogel exhibits a time-dependent increase in rigidity (Marudova-Zsivanovits *et al.* 2007), and the unconfined compressive strength along with the large-strain modulus of CrXG-soil composites similarly demonstrate gradual increases until convergence (Lee *et al.* 2023, Bang *et al.* 2024). However, the behavior of CrXG-soil composites at small strains remains insufficiently characterized.

This study evaluates the evolution of shear stiffness in CrXG-treated soils using bender element testing under varying curing times and sequential loading conditions. Two experimental approaches were employed. The first focused on the time-dependent development of shear stiffness, while the second examined vertical deformation behavior under sequential loading changes. Specimens were prepared with varying CrXG concentrations and cured for a minimum of 7 days to standardize curing effects. Additionally, environmental scanning electron microscopy (ESEM) was used to investigate the microstructural mechanisms responsible for stiffness variations due to CrXG treatment.

2. Materials and methods

2.1 Host soil: Jumunjin sand

Jumunjin sand was employed as the host soil in this study. Classified as poorly graded sand (SP), it exhibits a mean particle size (D_{50}) of 0.52 mm, a specific gravity (G_s)

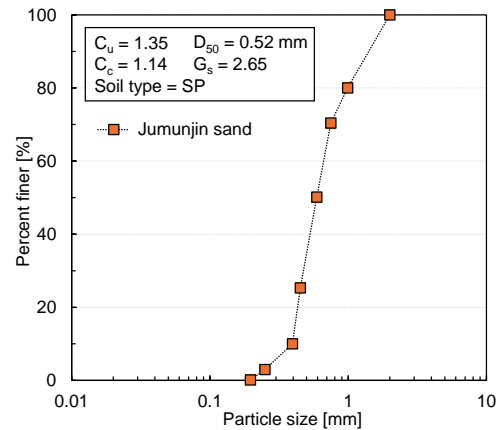


Fig. 1 Particle size distribution of Jumunjin sand

of 2.65, and both a coefficient of uniformity (C_u) of 1.35, and a coefficient of curvature (C_c) of 1.14. The particle size distribution is presented in Fig. 1.

2.2 Preparation of biopolymer treated soil specimen

This study focuses on CrXG, a composite synthesized from research-grade XG powder (CAS No. 11138-66-2; Merck, USA) and chromium nitrate nonahydrate ($\text{Cr}(\text{NO}_3)_3 \cdot 9\text{H}_2\text{O}$, CAS: 778902-08; Daejung Chemical Co., Korea). XG is a high-molecular-weight biopolymer produced by *Xanthomonas campestris* and is noted for its minimal environmental and health impacts. Its biodegradability, non-toxicity, and renewable microbial origin have led to its classification as an environmentally friendly material suitable for sustainable geotechnical engineering applications (Palaniraj and Jayaraman 2011, Soldo *et al.* 2020). Crosslinking XG with Cr^{3+} ions transforms the viscous XG gel into a rigid CrXG gel over time (Nolte *et al.* 1992). Sodium chloride (NaCl, CAS: 7647-14-5; Junsei, Korea) was incorporated to facilitate binding between XG and Cr^{3+} (Pelletier *et al.* 2001). In this study, the term “curing time” refers to the elapsed time during which Cr^{3+} -XG crosslinking reactions progress under constant water content conditions, leading to gradual gel stiffening and increased soil stiffness.

The CrXG hydrogel was prepared following the protocol outlined by Lee *et al.* (2023). Initially, XG powder was dissolved in deionized water at a mass ratio (m_b/m_w) of 5%. Separately, $\text{Cr}(\text{NO}_3)_3 \cdot 9\text{H}_2\text{O}$ and NaCl were dissolved in deionized water to form an aqueous Cr^{3+} solution. The two solutions were then blended to produce the CrXG hydrogel. This hydrogel was thoroughly mixed with soil that had been oven-dried at 110°C for 24 hours. All specimens were prepared at an initial water content of 20% and compacted to achieve a relative density in the range of 45–55%. CrXG concentrations of 0.25% and 1.00% were defined by the gravimetric ratio of binder mass to dry sand mass (m_b/m_s), and the hydrogel was mixed accordingly to achieve the specified content. The CrXG-treated soil was hand-compacted in three equal layers within an oedometer cell, with each layer receiving 20 uniform tamping strokes to ensure reproducible conditions.

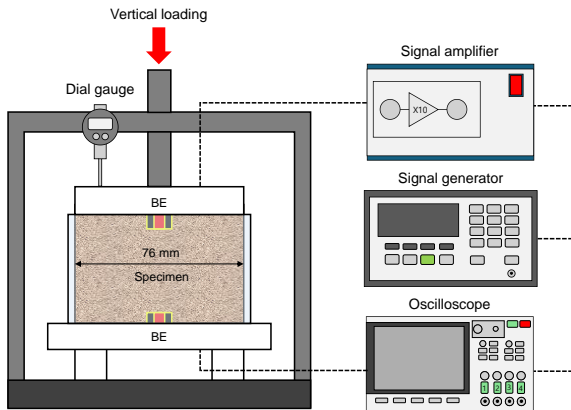


Fig. 2 Bender element test setup

2.3 Shear wave velocity measurement using bender element oedometer cell

Laboratory measurements of shear-wave velocity (V_s) were conducted in an oedometer cell constructed from acrylic tubes (76 mm in diameter and 70 mm in height) equipped with embedded bender element sensors, as shown in Fig. 2. Specimens were loaded vertically under K_0 conditions (i.e., with no lateral displacement). Gaps between the bender element insertion points and both the cell and cap were sealed with waterproofing Teflon tape to minimize water content fluctuations, including evaporation. Specimens were tested under partially saturated conditions, with an initial water content of 20%. No additional water was introduced during testing.

Bender elements typically consist of a metal plate with symmetrically arranged piezoelectric elements and external electrodes, often composed of nickel. They are classified as series or parallel based on the polarization direction of the piezoelectric elements (Lee and Santamarina 2005). In this study, a parallel-type bender element was installed on the source side to mitigate electrical interference from soil moisture, while a series-type element was used on the receiver side to capture a broad signal bandwidth (Lee and Santamarina 2005). The lower sensors were connected to a signal generator (Agilent 33120 A), which produced a single-step square wave with a 5 V amplitude at 1 kHz. A digital oscilloscope (Keysight DSO 6104A) recorded the input and output signals. Fig. 3 displays a typical shear wave signature, where the dotted square wave generated by the source propagates through the soil and is received as a solid line. Based on previous studies Lee and Santamarina (2005) (Fernandez 2000), the shear wave arrival time ($\Delta t_{tip-tip}$) is defined as the point at which the output wave transitions from the negative region to zero or positive values. The tip-to-tip distance (L) of the bender element is used as the travel distance, and shear-wave velocity is calculated using the following equation

$$V_s = \frac{L}{\Delta t_{tip-tip}} \quad (2)$$

2.4 Shear wave velocity measurement by curing time

The primary test investigated the influence of curing time on the shear wave velocity (V_s) of CrXG-treated soil specimens. Additionally, V_s was measured at different specimen depths to assess the uniformity of the crosslinking effects under consistent curing conditions. Two CrXG concentrations (0.25% and 1.00%) were evaluated under vertical stresses of 12.5, 200, and 400 kPa, with the vertical stress applied immediately after specimen setup in the oedometer cell. For each stress level, V_s and specimen height were recorded at curing intervals of 1 h, 6 h, 12 h, 1 d, 2 d, 4 d, and 7 d, with height measurements taken using a dial gauge to monitor settlement and volumetric deformation.

2.5 Shear wave velocity measurement under vertical stress

The secondary test aimed to assess the impact of confining pressure on volumetric deformation and shear wave velocity in CrXG-treated soils, relative to untreated soils. Experiments were conducted on 0.25% and 1.00% CrXG-treated soil samples that were cured for seven days to allow for sufficient stiffness development via time-dependent crosslinking (Lee *et al.* 2023). The testing protocol comprised two phases: loading and unloading. During the loading phase, specimens were subjected to incremental vertical loads of 12.5, 25, 50, 100, 200, 400, and 800 kPa. At each load increment, specimen height was measured with a dial gauge until the settlement rate stabilized at below 0.01 mm/min. Once stable, changes in height and shear wave arrival time were recorded. In the unloading phase, vertical stress was gradually reduced to 12.5 kPa in incremental steps. Similar to the loading phase, settlement was monitored, and measurements were taken only after the settlement rate stabilized at below 0.01 mm/min.

3. Results and discussions

3.1 Effect of curing time on shear wave velocity

Fig. 4 presents the vertical strain of CrXG-treated sand as a function of curing time under various applied vertical stresses. For a CrXG 0.25% (Fig. 4(a)), settlement due to vertical loading is completed within 1 hour at 12.5 kPa and 200 kPa, after which the settlement stabilizes. At 400 kPa, however, significant volume deformation continues until 12 hours, after which the settlement stabilizes. For a CrXG 1.00%, substantial settlement occurs within the first hour under all vertical stress levels. For 12.5 kPa, settlement remains constant thereafter, while at 200 kPa and 400 kPa, settlement continues until 6 and 12 hours, respectively, before stabilizing. Notably, higher CrXG content leads to greater settlement across all vertical stress levels compared to lower CrXG content.

Previous studies (Marudova-Zsivanovits *et al.* 2007, Lee *et al.* 2023) have identified three distinct stages of gelation in CrXG hydrogel and treated soils. In the initial stage, a rapid increase in rheological viscosity occurs as Cr^{3+} ions

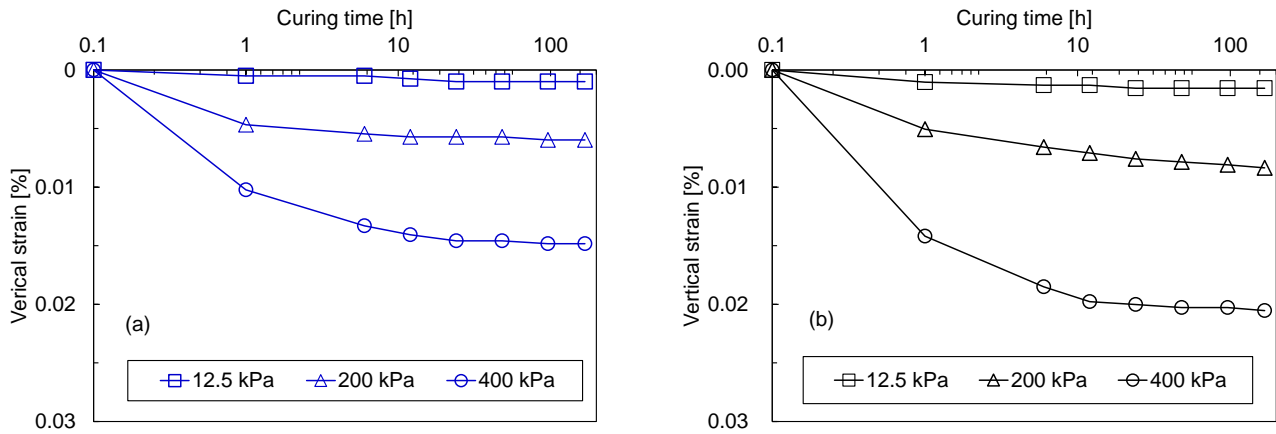


Fig. 4 Void ratio variation according to curing time (a) CrXG 0.25% (b) CrXG 1.00%

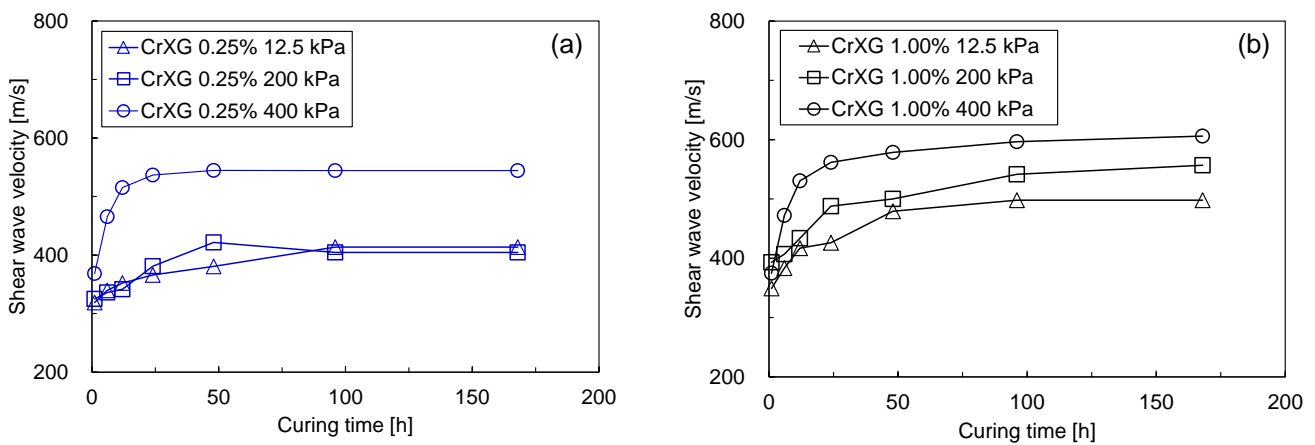


Fig. 5 Shear wave velocity variation according to curing time (a) CrXG 0.25% (b) CrXG 1.00%

initiate cluster formation with XG molecules. This is followed by a gradual increase in stiffness as a stable three-dimensional polymer network develops within the intergranular spaces.

Finally, a plateau phase is reached, indicating that the majority of crosslinking is complete; the hydrogel becomes highly rigid and exhibits reduced compressibility in soil.

Therefore, the evolution of shear wave velocity (V_s) and deformation behavior in CrXG-treated sand during testing was influenced by both the simultaneous application of vertical loading stress and the progression of CrXG hydrogel crosslinking, which induces a resisting force from gel stiffening. In the initial stage (up to 1 hour post-treatment), minimal gel stiffening left the soil relatively soft, resulting in pronounced settlement under vertical stress. As gel stiffening became significant after 6 hours, the resisting force effectively counteracted the applied stress, thereby reducing further settlement. Consequently, at vertical stresses of 12.5 kPa and 200 kPa, the hydrogel stabilized, and settlement became minimal. In contrast, at 400 kPa, the CrXG-treated soil exhibited sustained compressibility for up to 12 hours, indicating that initial gel stiffening was insufficient to stabilize settlement under high stress conditions. After 12 hours at 400 kPa, however, the

gel ultimately stiffened enough to suppress further settlement, leading to enhanced stabilization.

Fig. 5 illustrates the evolution of shear wave velocity (V_s) as a function of curing time and applied vertical stress for CrXG 0.25% and 1.00%. For a CrXG 0.25% (Fig. 5(a)), V_s increases gradually until 48 hours of curing, remaining constant until 168 hours across all vertical stresses. Notably, V_s values at 12.5 kPa and 200 kPa are nearly identical, suggesting that for low CrXG concentration, increasing the vertical load to 200 kPa has a minimal effect on stiffness. At 1 hour, the initial V_s values are 319 m/s, 325 m/s, and 369 m/s for 12.5 kPa, 200 kPa, and 400 kPa, respectively, indicating a higher initial stiffness response under 400 kPa.

For a CrXG 1.00% (Fig. 5(b)), the time-dependent increase in V_s is more pronounced. V_s increases until 48 hours of curing and then remains nearly constant from 48 to 168 hours across all vertical stress levels. After 1 hour, initial V_s values are 349 m/s, 375 m/s, and 393 m/s for 12.5 kPa, 200 kPa, and 400 kPa, respectively. When comparing both concentrations, the 1.00% CrXG-treated soil consistently exhibits higher V_s values under identical vertical stress conditions, implying that increased CrXG content enhances shear stiffness. In both cases, a significant increase in shear stiffness is observed after 48 hours (2

Table 1 Ultimate maximum shear modulus ($G_{max,ult}$) and rate factor (k')

CrXG concentration [mb/ms, %]	Vertical stress [kPa]	Estimated $G_{max,ult}$ [MPa]	Rate factor, k' [1/day]
0.25	12.5	246.91	64.96
	200	255.11	58.54
	400	507.25	20.12
1.00	12.5	447.33	79.15
	200	478.97	98.18
	400	564.68	45.81

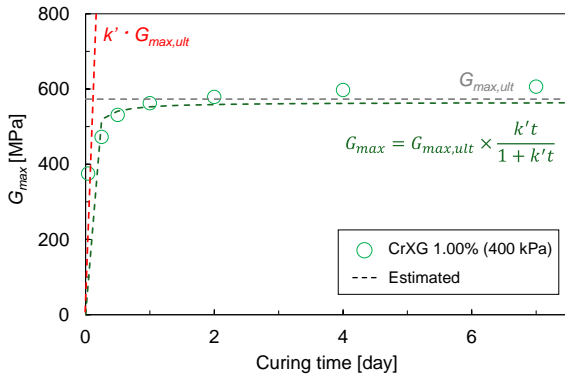


Fig. 6 Nonlinear development of maximum shear modulus with curing time

days), with full stabilization at approximately 168 hours (7 days). This initial stiffness increase is attributed to the progressive thickening of the three-dimensional hydrogel network through Cr–XG interactions, which enhances the hydrogel's structural integrity and increases its static yield stress (Lee *et al.* 2023).

The experimental results demonstrate that the V_s and G_{max} of CrXG-treated soils increases nonlinearly with curing time, with rapid stiffness gains in the first 48 hours and stabilization by 7 days. This behavior aligns with that observed in other stabilized soils, where time-dependent processes, such as crosslinking in CrXG (Lee *et al.* 2023, Bang *et al.* 2024) or hydration in cemented soils (Choo *et al.* 2017), govern stiffness development. The nonlinear increase in G_{max} is characterized using a hyperbolic model to estimate the long-term ultimate shear modulus ($G_{max,ult}$) as shown in Eq (4)

$$G_{max} = G_{max,ult} \times \frac{k't}{1 + k't} \quad (4)$$

where $G_{max,ult}$ is the ultimate shear modulus, t is the curing time, and k' is the rate factor representing the initial slope of the relationship between G_{max} and t . This model has been extensively used in previous studies to describe the time-dependent stiffness development in stabilized soils (Duncan and Chang 1970, Choo *et al.* 2017, Bang *et al.* 2024). By applying the hyperbolic model to the experimental data (Fig. 6), the study estimates $G_{max,ult}$ and assesses the rate of stiffness development under varying CrXG concentrations and vertical stress conditions.

Table 1 summarizes the $G_{max,ult}$ and k' values for the three applied vertical stresses and both CrXG

concentrations. The results indicate that $G_{max,ult}$ increases with higher vertical stress due to enhanced interparticle contact and improved interlocking between sand grains and the CrXG hydrogel, while k' decreases as the contribution of gel stiffening becomes less dominant under higher stresses. Additionally, at a given vertical stress, higher CrXG concentrations yield greater k' values, suggesting that increased CrXG content enhances the gel stiffening effect. For both 0.25% and 1.00% CrXG-treated soils, the ultimate G_{max} is achieved after 7 days of curing, indicating that a minimum curing period of 7 days is required to stabilize shear stiffness.

3.2 Effect of loading conditions on shear wave velocity

Fig. 7 illustrates the typical deformation behavior of soil specimens under both incremental and decremental vertical stresses. In untreated sand, vertical strain gradually decreases with increasing stress due to particle rearrangement (Fig. 7(a)). In contrast, CrXG-treated sand maintains stable vertical strain until a threshold is exceeded, at which point the stiffened gel structure begins to deform (Figs. 7(b) and 7(c)). Notably, once the yield vertical stress is reached, a significant reduction in vertical strain occurs for both 0.25% and 1.00% CrXG-treated sands. The yield vertical stress increases with CrXG concentration, ranging from approximately 50–100 kPa for 0.25% CrXG to 100–200 kPa for 1.00% CrXG.

BE tests conducted over various curing times confirmed that CrXG-treated soils achieve constant stiffness after 7 days. However, the mechanical response—specifically, shear wave velocity (V_s) and deformation behavior—varies considerably under different vertical stress conditions. At low vertical stresses, the behavior of cemented soils is primarily governed by interparticle cementation, while at high vertical stresses, the response becomes stress-controlled (Yun and Santamarina 2005, Cha *et al.* 2014). This stress-dependent behavior is consistent with previous studies on stabilized soils, where the relationship between vertical strain and stress serves as a key indicator of deformation evolution and potential collapse (Yun and Santamarina 2005, Feda 2013). In this study, the deformation patterns of CrXG-treated soils are examined to further elucidate the role of vertical stress in governing their mechanical behavior.

Fig. 8 illustrates applied vertical stress and shear wave velocity in loading and unloading phase for untreated sand, CrXG 0.25%, and 1.00% treated sand. V_s can be expressed

by the power function of the vertical effective stress, σ'_v , shown on Eq. (5) (Roesler 1979, Santamarina *et al.* 2001)

$$V_s = \alpha \left(\frac{\sigma'_v}{1 \text{ kPa}} \right)^\beta \quad (5)$$

where α represents the shear wave velocity at a vertical stress of 1 kPa, and β is an exponent that reflects the sensitivity of V_s to changes in vertical effective stress. This relationship holds when capillary forces are negligible compared to stress-induced skeletal forces (Roesler 1979, Santamarina *et al.* 2001, Cha *et al.* 2014, Kim *et al.* 2023, Park *et al.* 2023, Kim *et al.* 2024).

During the loading phase (Fig. 8(a)), the untreated specimen exhibited the lowest α value of 42.09 m/s, whereas the CrXG-treated specimens recorded α values of 214 m/s for 0.25% CrXG and 362 m/s for 1.00% CrXG. At low vertical stresses, higher CrXG concentrations yield higher V_s values. Furthermore, untreated soil demonstrated the highest sensitivity, with a β value of 0.1588, followed by 0.1526 for 0.25% CrXG and 0.0719 for 1.00% CrXG. These results suggest that untreated soil exhibits the greatest variation in V_s with increasing stress, while higher CrXG concentrations diminish the effect of stress on V_s . In soils cured for over 7 days, significant gel stiffening between sand particles results in high V_s values at low vertical stresses, so that incremental stress application influences V_s more than the inherent gel stiffening. The decrease in β with increasing CrXG concentration indicates a shift in stiffness dominance from hydrogel effects to stress-induced particle interlocking.

In unloading phase, untreated sand recorded the lowest α value at 26.86 m/s, with 181.87 m/s for 0.25% CrXG and 274.84 m/s for 1.00% CrXG. The α values during unloading were consistently lower than those observed during loading for all specimens. The β value during unloading was highest for untreated sand at 0.2164, with reduced sensitivity for 0.25% CrXG (0.1738) and the lowest for 1.00% CrXG (0.1016). This difference in α and β values between loading and unloading stages may be explained by partial structural degradation that occurred during the loading phase. Exposure to the maximum vertical stress likely caused microstructural adjustments, such as slight breakdown of the CrXG hydrogel network or rearrangement of particle contacts, leading to reduced initial stiffness and greater stress sensitivity during unloading. Overall, the β values in the unloading phase are higher than those in the loading phase, indicating a steeper decrease in stiffness upon unloading.

Various models exist for predicting shear wave velocity under different stress conditions. In this study, the effective vertical stress method was employed without explicitly considering K_0 conditions (Eq. (6)). This model confirms that coarse, dense soils exhibit higher velocities at low stresses (high α) but lower sensitivity to stress changes (low β) due to smaller variations in density and coordination number with increasing stress. Eq. 6 represents the inverse relationship between the α -factor and β -exponent for soils, including clays and sands (Salva Ramirez *et al.* 2023)

$$V_s = \alpha \left(\frac{\sigma'_v}{1 \text{ kPa}} \right)^\beta \quad (6)$$

Previous studies have established that, for contact deformation at constant fabric, β values can be justified as follows (Cascante and Santamarina 1996): $\beta = 0$ for an ideal solid; $\beta \approx 0$ for cemented granular media; and $\beta = 1/6$ for Hertzian contacts (elastic spherical particles). More compressible soils exhibit higher β exponents—even with identical contact characteristics—due to fabric changes and increased coordination numbers during loading (Santamarina 2001). Experimental findings typically report β values ranging from 0.70 to 0.85 for clay and from 0.10 to 0.55 for sand. Moreover, cemented sand generally exhibits β values near zero, reflecting the absence of micro fissures or debonding, while the parameter α increases with the degree of cementation (Cha 2014).

Fig. 9 presents the α -factor and β -exponent for both untreated and CrXG-treated sand, along with the inverse trend line relationship. The data indicate that untreated sand falls within the expected range of the shear wave velocity model for sand. For CrXG-treated sand at a 0.25% concentration, the observed β value is comparable to that of untreated sand; however, its higher α value places it closer to the range associated with cemented sand rather than clay. As the CrXG concentration increases, both the α -factor and β -exponent shift into the range characteristic of cemented sand (Yun and Santamarina 2005, Fernandez 2001), suggesting that CrXG treatment influences interparticle contacts and fabric structure in a manner similar to cemented soils.

This trend is further corroborated by ESEM observations (Fig. 10). In untreated sand, no bonding is observed between particles, whereas CrXG-treated sand at a 1.00% concentration (Fig. 10(b)) exhibits a thick hydrogel fabric forming between particles. At higher CrXG concentrations, the denser and stiffer hydrogel fabric promotes stronger interparticle bonding, enhancing soil stiffness in a fashion akin to cemented soils. However, despite the observed decrease in β with increasing α , CrXG-treated soil does not fully replicate the mechanical behavior or volumetric deformation characteristics of cemented soils. This discrepancy arises from the inherent stiffness differences between the soft-elastic hydrogel and traditional cementitious bonding materials. These results demonstrate that CrXG-treated sand exhibits shear wave velocity characteristics and α - β parameter trends that closely resemble those of cemented sands, particularly at higher concentrations. Compared to other biopolymer-treated soils such as those stabilized with untreated XG or gellan gum (Chang *et al.* 2015, Soldo *et al.* 2020), CrXG-treated sand shows superior stiffness retention under vertical stress, suggesting its potential as a sustainable alternative to conventional cement-based stabilization.

3.3 Implications and limitations

This study demonstrates that the application of CrXG to sandy soils enhances shear stiffness through gel stiffening and effectively stabilizes settlement. Previous research has shown that CrXG-treated soils exhibit high compressive strength and cohesion in submerged or hydrated states, contributing significantly to seepage control, improved

ultimate bearing capacity (Lee *et al.* 2023), and enhanced liquefaction resistance. Consequently, CrXG-treated soil shows promise as a backfill material for submerged or shallow-depth structures such as sewer or power plant pipelines. However, under dry conditions, CrXG-treated sandy soils may experience diminished durability and shear stiffness (Bang *et al.* 2024). To broaden its applicability across varied ground conditions, further research is required to address and mitigate these limitations. Furthermore, while the laboratory findings confirm the mechanical benefits of CrXG treatment, the practical feasibility of implementing this technique on a large scale remains to be explored. Key considerations such as material cost, large-scale mixing and injection techniques, equipment requirements, and quality control in field environments are essential for real-world application.

It should also be noted that the curing period in this study was limited to 7 days, corresponding to the stabilization of initial stiffness. However, long-term durability and stiffness retention under environmental conditions such as repeated wet-dry cycles, microbial degradation, and hydrogel swelling remain important considerations. While previous studies have reported improved resistance of CrXG-treated soils to moisture-induced deterioration (Lee *et al.* 2023, Bang *et al.* 2024), further research is needed to systematically investigate their mechanical stability over extended periods in realistic field environments.

4. Conclusions

This study investigated the small-strain shear stiffness evolution along curing process and vertical deformation behavior and V_s - σ'_v relationship parameters of CrXG-treated soil by assessing shear wave velocity through bender element test. The key findings are summarized as follows:

- CrXG-treated soil exhibited a nonlinear increase in shear stiffness over time, primarily due to the progressive gel stiffening effect. Higher CrXG concentrations facilitated greater initial shear stiffness during the early curing stages, with stiffness stabilization occurring after approximately 7 days.
- The compressibility of CrXG hydrogels varied with vertical stress levels. At lower vertical stress, settlement stabilized within one hour, whereas at higher vertical stress, settlement continued for up to 12 hours before stabilization due to gel stiffening. Additionally, higher CrXG concentrations increased the yield vertical stress, indicating enhanced resistance to volumetric deformation and hydrogel collapse under sustained loading.
- The V_s of CrXG-treated soils increased with both vertical stress and CrXG concentration. Higher CrXG concentrations resulted in greater V_s values, with the α -factor and β -exponent aligning more closely with those of typical cemented soils. This behavior is attributed to the formation of an intergranular hydrogel matrix that effectively bonds sand particles, enhancing overall soil stiffness.

While this study demonstrated that CrXG treatment enhances the small-strain stiffness of sand, the findings are limited in scope. To fully understand the long-term stiffness and deformation behavior of CrXG-treated soils, future research should explore extended curing durations across various soil conditions, incorporating more realistic loading scenarios representative of geotechnical engineering applications. In addition, future research should assess the field-scale feasibility and cost-effectiveness of CrXG treatment to support its transition from laboratory studies to practical applications.

Acknowledgments

This research was financially supported by the Ministry of Oceans and Fisheries (MOF) of the Korean Government (Project No. 20220364), and the National Research Foundation of Korea (NRF) grant funded by the Korea government (MSIT) (No. 2023R1A2C300559611).

References

- Amaral, M.F., Da Fonseca, A.V., Arroyo, M., Cascante, G. and Carvalho, J. (2011), "Compression and shear wave propagation in cemented-sand specimens", *Géotechnique Lett.*, **1**(3), 79-84. <https://doi.org/10.1680/geolett.11.00032>.
- Anochie-Boateng, J.K. and Tutumluer, E. (2014), "Advanced testing and characterization of shear modulus and deformation characteristics of oil sand materials", *J. Test. Eval.*, **42**(5), 1228-1239. <https://doi.org/10.1520/JTE20130049>.
- ASTM. (2017), *Standard test methods for particle-size distribution (gradation) of soils using sieve analysis*. ASTM International.
- ASTM. (2019), *Standard test methods for laboratory determination of water (moisture) content of soil and rock by mass*. ASTM International.
- Atkinson, J. (2000), "Non-linear soil stiffness in routine design", *Géotechnique.*, **50**(5), 487-508. <https://doi.org/10.1680/geot.2000.50.5.487>.
- Bang, J.U., Lee, M., Park, D.Y., Chang, I. and Cho, G.C. (2024), "Effects of soil composition and curing conditions on the strength and durability of cr3+-crosslinked biopolymer-soil composites", *Constr. Build. Mater.*, **449**, 138440. <https://doi.org/10.1016/j.conbuildmat.2024.138440>.
- Bekkouche, S.R., Benzerara, M., Zada, U., Muhammad, G. and Ali, Z. (2022), "Use of eco-friendly materials in the stabilization of expansive soils", *Buildings*, **12**(10), 1770. <https://doi.org/10.3390/buildings12101770>.
- Bezuijen, A., Van Der Zon, W. and Talmon, A. (2005), "Laboratory testing of grout properties and their influence on backfill grouting", ITA World Tunnel Congress 2005-Underground Space Use. Analysis of the Past and Lessons for the Future.
- Boaventura, N.F., Sousa, T.F.d.P. and Casagrande, M.D.T. (2023), "The application of an eco-friendly synthetic polymer as a sandy soil stabilizer", *Polymers*, **15**(24), 4626. <https://doi.org/10.3390/polym15244626>.
- Bouazza, A., Gates, W.P. and Ranjith, P.G. (2009), "Hydraulic conductivity of biopolymer-treated silty sand", *Géotechnique*, **59**(1), 71-72. <https://doi.org/10.1680/geot.2007.00137>.
- Budhu, M. (2010), *Soil mechanics and foundations*, John Wiley and Sons.
- Cabalar, A.F., Wiszniewski, M. and Skutnik, Z. (2017), "Effects of

- xanthan gum biopolymer on the permeability, odometer, unconfined compressive and triaxial shear behavior of a sand”, *Soil Mech. Found. Eng.*, **54**, 356-361. <https://doi.org/10.1007/s11204-017-9481-1>.
- Cha, M., Santamarina, J.C., Kim, H.S. and Cho, G.C. (2014), “Small-strain stiffness, shear-wave velocity, and soil compressibility”, *J. Geotech. Geoenviron. Eng.*, **140**(10), 06014011. [https://doi.org/10.1061/\(ASCE\)GT.1943-5606.0001157](https://doi.org/10.1061/(ASCE)GT.1943-5606.0001157).
- Chakraborty, S., Banerjee, A., Das, J.T., Mosadegh, L. and Puppala, A.J. (2018), Impact of variation of small strain shear modulus on seismic slope stability analysis of a levee: A sensitivity analysis,
- Chang, I., Im, J., Prasadhi, A.K. and Cho, G.C. (2015), “Effects of xanthan gum biopolymer on soil strengthening”, *Constr. Build. Mater.*, **74**, 65-72. <https://doi.org/10.1016/j.conbuildmat.2014.10.026>.
- Chang, I., Lee, M., Tran, A.T.P., Lee, S., Kwon, Y.M., Im, J. and Cho, G.C. (2020), “Review on biopolymer-based soil treatment (bpst) technology in geotechnical engineering practices”, *Transport. Geotech.*, **24**, 100385. <https://doi.org/10.1016/j.trgeo.2020.100385>.
- Chen, C., Habert, G., Bouzidi, Y. and Jullien, A. (2010), “Environmental impact of cement production: Detail of the different processes and cement plant variability evaluation”, *J. Cleaner Product.*, **18**(5), 478-485. <https://doi.org/10.1016/j.jclepro.2009.12.014>.
- Choo, H., Nam, H. and Lee, W. (2017), “A practical method for estimating maximum shear modulus of cemented sands using unconfined compressive strength”, *J. Appl. Geophys.*, **147**, 102-108. <https://doi.org/10.1016/j.jappgeo.2017.10.012>.
- Consoli, N.C., Viana da Fonseca, A., Cruz, R.C. and Heineck, K.S. (2009), “Fundamental parameters for the stiffness and strength control of artificially cemented sand”, *J. Geotech. Geoenviron. Eng.*, **135**(9), 1347-1353. [https://doi.org/10.1061/\(ASCE\)GT.1943-5606.0000000](https://doi.org/10.1061/(ASCE)GT.1943-5606.0000000).
- Duncan, J.M. and Chang, C.Y. (1970), “Nonlinear analysis of stress and strain in soils”, *J. Soil Mech. Found. Division*, **96**(5), 1629-1653. <https://doi.org/10.1061/JSFEAQ.0001458>.
- Fernandez, A.L. (2000), Tomographic imaging the state of stress, Georgia Institute of Technology.
- Ghorbani, A. and Salimzadehshooiili, M. (2019), “Dynamic characterization of sand stabilized with cement and rha and reinforced with polypropylene fiber”, *J. Mater. Civil Eng.*, **31**(7), 04019095. [https://doi.org/10.1061/\(ASCE\)MT.1943-5533.0002727](https://doi.org/10.1061/(ASCE)MT.1943-5533.0002727).
- Gu, X., Yang, J., Huang, M. and Gao, G. (2015), “Bender element tests in dry and saturated sand: Signal interpretation and result comparison”, *Soils Found.*, **55**(5), 951-962. <https://doi.org/10.1016/j.sandf.2015.09.002>.
- Hoyos, L.R., Suescún-Florez, E.A. and Puppala, A.J. (2015), “Stiffness of intermediate unsaturated soil from simultaneous suction-controlled resonant column and bender element testing”, *Eng. Geol.*, **188**, 10-28. <https://doi.org/10.1016/j.enggeo.2015.01.014>.
- Huang, J., Kogbara, R.B., Hariharan, N., Masad, E.A. and Little, D.N. (2021), “A state-of-the-art review of polymers used in soil stabilization”, *Constr. Build. Mater.*, **305**, 124685. <https://doi.org/10.1016/j.conbuildmat.2021.124685>.
- Kim, N., Lee, J.S., Park, G., Yoo, Y. and Park, J. (2024), “Evolution of relative density and shear wave velocity in non-compacted embankment layers: Geological long-term monitoring”, *Eng. Geol.*, **340**, 107674. <https://doi.org/10.1016/j.enggeo.2024.107674>.
- Kim, S.Y., Chun, J.K., Yeo, J.Y. and Lee, J.S. (2023), “Estimation of soil porosity in mine tailing using parameters from instrumented oedometer test”, *Eng. Geol.*, **317**, 107065. <https://doi.org/10.1016/j.enggeo.2023.107065>.
- Kwon, Y.M., Chang, I. and Cho, G.C. (2023), “Consolidation and swelling behavior of kaolinite clay containing xanthan gum biopolymer”, *Acta Geotechnica*, **18**(7), 3555-3571. <https://doi.org/10.1007/s11440-023-01794-8>.
- Latifi, N., Horpibulsuk, S., Meehan, C.L., Abd Majid, M.Z., Tahir, M.M. and Mohamad, E.T. (2017), “Improvement of problematic soils with biopolymer—an environmentally friendly soil stabilizer”, *J. Mater. Civil Eng.*, **29**(2), 04016204. [https://doi.org/10.1061/\(ASCE\)MT.1943-5533.0001706](https://doi.org/10.1061/(ASCE)MT.1943-5533.0001706).
- Lee, J.S. and Santamarina, J.C. (2005), “Bender elements: Performance and signal interpretation”, *J. Geotech. Geoenviron. Eng.*, **131**(9), 1063-1070. [https://doi.org/10.1061/\(ASCE\)1090-0241\(2005\)131:9\(1063\)](https://doi.org/10.1061/(ASCE)1090-0241(2005)131:9(1063)).
- Lee, M., Chang, I. and Cho, G.C. (2023), “Advanced biopolymer-based soil strengthening binder with trivalent chromium-xanthan gum crosslinking for wet strength and durability enhancement”, *J. Mater. Civil Eng.*, **35**(10), 04023360. <https://doi.org/10.1061/JMCEE7.MTENG-16123>.
- Lee, M., Chang, I., Park, D.Y. and Cho, G.C. (2023), “Strengthening and permeability control in sand using cr3+-crosslinked xanthan gum biopolymer treatment”, *Transport. Geotech.*, **43**, 101122. <https://doi.org/10.1016/j.trgeo.2023.101122>.
- Lee, M., Kwon, Y.M., Park, D.Y., Chang, I. and Cho, G.C. (2022), “Durability and strength degradation of xanthan gum based biopolymer treated soil subjected to severe weathering cycles”, *Sci. Rep.*, **12**(1), 19453. <https://doi.org/10.1038/s41598-022-23823-4>.
- Lee, S., Chang, I., Chung, M.K., Kim, Y. and Kee, J. (2017), “Geotechnical shear behavior of xanthan gum biopolymer treated sand from direct shear testing”, *Geomech. Eng.*, **12**(5), 831-847. <https://doi.org/10.12989/gae.2017.12.5.831>.
- Liu, L., Deng, T., Deng, Y., Zhan, L., Horpibulsuk, S. and Wang, Q. (2022), “Stabilization nature and unified strength characterization for cement-based stabilized soils”, *Constr. Build. Mater.*, **336**, 127544. <https://doi.org/10.1016/j.conbuildmat.2022.127544>.
- Marudova-Zsivanovits, M., Jilov, N. and Gencheva, E. (2007), “Rheological investigation of xanthan gum-chromium gelation and its relation to enhanced oil recovery”, *J. Appl. Polymer Sci.*, **103**(1), 160-166. <https://doi.org/10.1002/app.25025>.
- Mendonça, A., Morais, P.V., Pires, A.C., Chung, A.P. and Oliveira, P.V. (2020), “A review on the importance of microbial biopolymers such as xanthan gum to improve soil properties”, *Appl. Sci.*, **11**(1), 170. <https://doi.org/10.3390/app11010170>.
- Mitchell, J. (2005), Fundamentals of soil behavior, John Wiley & Sons/John Wiley & Sons, LTD.
- Murthy, V. (2002), Geotechnical engineering: Principles and practices of soil mechanics and foundation engineering, CRC press.
- Noh, D.H., Ajo-Franklin, J.B., Kwon, T.H. and Muhunthan, B. (2016), “P and S wave responses of bacterial biopolymer formation in unconsolidated porous media”, *J. Geophys. Res.: Biogeosci.*, **121**(4), 1158-1177. <https://doi.org/10.1002/2015JG003118>.
- Nolte, H., John, S., Smidsrød, O. and Stokke, B.T. (1992), “Gelation of xanthan with trivalent metal ions”, *Carbohydrate Polymers*, **18**(4), 243-251. [https://doi.org/10.1016/0144-8617\(92\)90089-9](https://doi.org/10.1016/0144-8617(92)90089-9).
- Oh, T.M., Bang, E.S., Cho, G.C. and Park, E.S. (2017), “Estimation of undrained shear strength for saturated clay using shear wave velocity”, *Mar. Georesour. Geotec.*, **35**(2), 236-244. <https://doi.org/10.1080/1064119X.2016.1140855>.
- Palaniraj, A. and Jayaraman, V. (2011), “Production, recovery and applications of xanthan gum by *Xanthomonas campestris*”, *J. Food Eng.*, **106**(1), 1-12.

- <https://doi.org/10.1016/j.jfoodeng.2011.03.035>.
- Park, J., Kim, S.Y., Hoang, Q.N. and Lee, J.S. (2023), "Impact of diatoms on the load-deformation response of marine sediments during drained shear: Small-to-large strain stiffness", *Eng. Geol.*, **315**, 107006. <https://doi.org/10.1016/j.enggeo.2023.107006>.
- Park, S.S., Moon, H.D. and Park, S.H. (2015), "A study on dynamic analyses of cut and cover tunnel during earthquakes", *J. Eng. Geol.*, **25**(2), 237-250. <https://doi.org/10.9720/kseg.2015.2.237>.
- Pelletier, E., Viebke, C., Meadows, J. and Williams, P. (2001), "A rheological study of the order-disorder conformational transition of xanthan gum", *Biopolymers: Original Research on Biomolecules*, **59**(5), 339-346. [https://doi.org/10.1002/1097-0282\(20011015\)59:5<339::AID-BIP1031>3.0.CO;2-A](https://doi.org/10.1002/1097-0282(20011015)59:5<339::AID-BIP1031>3.0.CO;2-A).
- Pitilakis, K. and Tsiniadis, G. (2013), *Performance and seismic design of underground structures*, Springer.
- Roesler, S.K. (1979), "Anisotropic shear modulus due to stress anisotropy", *J. Geotech. Eng. Division*, **105**(7), 871-880. <https://doi.org/10.1061/AJGEB6.0000835>.
- Salva Ramirez, M., Park, J., Terzariol, M., Jiang, J. and Santamarina, J.C. (2023), "Shallow seafloor sediments: Density and shear wave velocity", *J. Geotech. Geoenviron. Eng.*, **149**(5), 04023022. <https://doi.org/10.1061/JGGEFK.GTENG-1075>.
- Santamarina, J.C., Klein, A. and Fam, M.A. (2001), "Soils and waves: Particulate materials behavior, characterization and process monitoring", *J. Soils Sediments*, **1**(2), 130. <https://doi.org/10.1007/BF02987719>.
- Seo, S., Lee, M., Im, J., Kwon, Y.M., Chung, M.K., Cho, G.C. and Chang, I. (2021), "Site application of biopolymer-based soil treatment (bpst) for slope surface protection: In-situ wet-spraying method and strengthening effect verification", *Constr. Build. Mater.*, **307**, 124983. <https://doi.org/10.1016/j.conbuildmat.2021.124983>.
- Soldo, A., Miletic, M. and Auad, M.L. (2020), "Biopolymers as a sustainable solution for the enhancement of soil mechanical properties", *Sci. Rep.*, **10**(1), 267. <https://doi.org/10.1038/s41598-019-57135-x>.
- Yun, T.S. and Santamarina, J.C. (2005), "Decementation, softening, and collapse: Changes in small-strain shear stiffness in k₀ loading", *J. Geotech. Geoenviron. Eng.*, **131**(3), 350-358. [https://doi.org/10.1061/\(ASCE\)1090-0241\(2005\)131:3\(350\)](https://doi.org/10.1061/(ASCE)1090-0241(2005)131:3(350)).